Cellular Signalling 63 (2019) 109389

Contents lists available at ScienceDirect

Cellular Signalling

journal homepage: www.elsevier.com/locate/cellsig

Delta/notch-like epidermal growth factor-related receptor promotes stemness to facilitate breast cancer progression

Lijun Wang[a,1], Qi Wu[a,e,f,1], Zhiyu Li[a], Si Sun[b], Jingping Yuan[c], Juanjuan Li[a], Yimin Zhang[a], Dehua Yu[c,d], Changhua Wang[d,**,1], Shengrong Sun[d,*,1]

[a] Department of Breast and Thyroid Surgery, Renmin Hospital of Wuhan University, Wuhan, Hubei, PR China
[b] Department of Clinical Laboratory, Renmin Hospital of Wuhan University, Wuhan, Hubei, China
[c] Department of Pathology, Renmin Hospital of Wuhan University, Wuhan, Hubei, PR China
[d] Department of Pathophysiology, Wuhan University School of Basic Medical Sciences, Wuhan, Hubei, PR China
[e] Metabolomics and Cell Biology Platforms, Gustave Roussy Comprehensive Cancer Institute, Villejuif, France
[f] Faculty of Medicine, University of Paris Sud, Kremlin-Bicêtre, France

ARTICLE INFO

Keywords:
DNER
Breast cancer
Proliferation
Metastasis
Girdin/PI3K/AKT axis

ABSTRACT

DNER, Delta/Notch-like epidermal growth factor (EGF)-related receptor, is a neuron-specific transmembrane protein carrying extracellular EGF-like repeats. The function of DNER in breast cancer has not been evaluated. The present study demonstrates that the expression of DNER in breast cancer tissue is significantly higher than its expression in breast benign disease and is associated with poor recurrence-free survival (RFS) of breast cancer patients. It demonstrated that DNER could enhance the proliferation and metastasis of breast cancer cells in vitro and significantly increases tumor growth in vivo. Our study uncovered that DNER can promote breast cancer cells proliferation and metastasis by activating Girdin/PI3K/AKT signaling and subsequently regulating several key genes involving the characters of cancer stem cells. Taken together, DNER promotes breast cancer growth and metastasis, which provided a theoretical basis for future applications of DNER inhibitors in the treatment of breast cancer.

1. Introduction

Breast cancer is a significant health problem and it is the second leading cause of cancer-related death in women in China, approximately one in every ten women will develop the disease in their lifetime [1]. A hallmark of cancer stem cells (CSCs) is the presence of self-renewal and multipotential differentiation, in which several highly conserved signal transduction pathways involved in development and tissue homeostasis including the Notch, Hedgehog, and Wnt pathways are found to be persistently activated [2]. In addition, the ability of CSCs contributes to the growth, metastasis, recurrence and drug resistance of cancer [3]. Therefore, researchers will continue to explore factors that target these pathways to control stem-cell replication, survival and differentiation with the aim of finding treatment strategies of breast cancer.

The continual activation of Notch signaling can lead to abnormalities in the signaling pathway and then regulate the process of cell-fate decisions during breast cancer progression [4,5]. Constitutive Notch proteins are large transmembrane proteins and can be activated by the direct interaction of Notch ligands expressed on apposed cells such as DSL (Delta, Serrate and Lag) family members. There are share repeated EGF-like motifs in their extracellular regions between Notch and DSL family members for physiological interactions. Delta/Notch-like EGF-related receptor (DNER, also named HE60) is a transmembrane protein

Abbreviations: DNER, Delta/notch-like epidermal growth factor-related receptor; CSCs, cancer stem cells; MTT, methyl thiazolyl tetrazolium; GAPDH, Glyceraldehyde-3-phosphate dehydrogenase; IHC, immunohistochemistry; QDs, Quantum dots; HRs, hazard ratios; PR, progesterone receptor; HER2, human epithelial growth factor receptor-2; ER, estrogen receptor; TCGA, The Cancer Genome Atlas; RFS, recurrence-free survival; IPA, ingenuity pathway analysis; EMT, epithelial-mesenchymal transition; HDAC, histone deacetylase; NICD, Notch intracellular domain; DSL, Delta, Serrate, Lag2; EGFR, epidermal growth factor receptor; GPCRs, G-protein coupled receptors.

* Correspondence to: S. Sun, Department of Breast and Thyroid Surgery, Renmin Hospital of Wuhan University, 99 Zhang Zhidong Road, Wuhan 430060, Hubei Province, PR China.
** Corresponding to: C. Wang, Department of Pathophysiology, Wuhan University School of Basic Medical Sciences, Wuhan 430060, Hubei Province, PR China.
E-mail addresses: chwang0525@whu.edu.cn (C. Wang), sun137@sina.com (S. Sun).
[1] These authors contributed equally to this work.

https://doi.org/10.1016/j.cellsig.2019.109389
Received 27 February 2019; Received in revised form 8 August 2019; Accepted 9 August 2019
Available online 10 August 2019

carrying extracellular EGF-like repeats and specifically expressed in somatodendritic regions of the cerebellum [6,7]. However, DNER lacks the DSL binding domain which is perceived as the essential of Notch ligands [8,9]. Although there is some structural difference, DNER is identified as a Notch ligand mediating cell–cell interaction [8]. In fact, it has been reported that DNER may be a double-facet factor in cancer progression: we demonstrated that DNER played an important impact on cell transformation in several cancer cells, and the growth could also significantly reduced through silencing DNER in a previous work [10,11], but functions as a tumor suppressor in glioblastoma [12]. The dual role of DNER suggests that its function is tissue-specific, and no previous study has investigated the roles of DNER in breast cancer.

Girdin (Gα-interacting vesicle-associated protein), is a multi-domain protein which is required for growth factors such as EGF [13,14], insulin [15] and VEGF [16] to enhance AKT activation in a PI3K-dependent manner [17]. The previous study demonstrated that Girdin is a substrate for tyrosine kinases and directly binds ligand-activated EGFR to enhance autophosphorylation and activate AKT in a PI3K-dependent manner [17]. Besides, the intracellular carboxyl terminus of DNER comprises 70 amino acids, with a potential phosphorylation site by tyrosine kinases [7]. Working downstream of DNER, Girdin may enhance PI3K/AKT signals during cancer invasion and metastasis.

Taken together, our results suggest that DNER could be of potential interest for regulating the growth and metastasis of breast cancer cells through activating Girdin/PI3K/AKT signaling pathway and modulating the primary genes of cancer stem cells.

2. Materials and methods

2.1. Ethics approval

Human samples were obtained from Renmin Hospital of Wuhan University. The study was approved by the Institutional Ethics Committee of Renmin Hospital of Wuhan University. All methods were performed in accordance with relevant guidelines and local regulations. In addition, the animals were handled according to the protocol approved by the Institutional Animal Care and Use Committee of Renmin Hospital of Wuhan University. All procedures performed in studies involving human participants were in accordance with the 1964 Helsinki declaration and its later amendments or comparable ethical standards.

2.2. Informed consent

All patients included in the study provided written informed consent. Patients did not receive financial compensation.

2.3. Cell lines and antibodies

Human breast cancer cell line, MCF-7, MDA-MB-231, MDA-MB-468, ZR-75-30, MCF-10A, HCC-1937 cell were from ATCC (Manassas, VA) and cultured according to their protocols. GAPDH (dilution 1:1000), AKT (dilution 1:1000), Phospho-AKT (Ser473) (dilution 1:500) were purchased from Cell Signaling Technology and DNER (dilution 1:500) antibody were purchased from Biorbyt (Cambridge, UK). CDH1 (dilution 1:1000),CCND1 (dilution 1:1000), and HES1 (dilution 1:500) antibody were purchased from Abcam Girdin, p-Try, p85α were purchased from Santa Cruz Biotechnology (dilution 1:500). Polypotent growth factor (PTN) was purchased from HZbscience (ZY309Bo012) SC79 the activator of AKT was purchased from Abcam (ab146428).

2.4. Cell viability assay

The methyl thiazolyl tetrazolium (MTT) (Amresco, Solon, OH, USA) was dissolved in phosphate buffered saline(PBS) at a concentration of 5 mg/ml, filtered, and stored at 4 °C. The cells were seeded into a 96-well plate at 4000 cells per well in the DMEM containing 10% FBS. After 12 h, the medium was replaced with serum-free DMEM-Free Glucose overnight. MDA-MB-231 Cells were treated with control siRNA lentiviruses and DNER siRNA lentiviruses for 3 days and MCF-7 cells were transfected with control vector or Flag-DNER plasmid for same times. For the viability assay, 20 μl MTT was added into each well. The absorbance at 570 nm was measured using an ELISA reader (Biotek, Winooski, Vermont, USA) and used to determine relative cell numbers in each well. The viability of control cells was 100%.

2.5. Cell cycle assay

The analysis of cell cycle was used by Cell Cycle Analysis Kit (BD Biosciences, San Jose, CA) and measured according to their protocols. Breast cancer cells ($5.0*10^5$ cells per well) were cultured in 6 well/plates and allowed to adhere to the well walls for 12 h. After starvation overnight, two kind of cells were respectively treated with control siRNA lentiviruses and DNER siRNA lentiviruses or Flag-DNER plasmid and control vector for 72 h. Subsequently, the cells were collected, washed in PBS and fixed in 70% ethanol at 4 °C overnight. Then, the cells were centrifuged at 2000 rpm for 5 min at 4 °C temperature. The supernatant was removed and the cells were resuspended in 4 mL of PBS and centrifuged again. The supernatant was removed and the cell pellet was 100 μl RNase A incubating for 30 min at 37 °C. Finally, 400 μl PI (propidium iodide) was added and the cells were incubated for an additional 30 min in the dark at 37 °C. The cell cycle distribution was determined by flow cytometry for DNA content (FACScan, Becton Dickinson, Germany). Results were presented as percentage of breast cancer cells in different phases of cell cycle (G0-G1, S and G2-M) in relation to total number of cells counted.

2.6. Cell migration assay

Breast cancer cells MCF-7 and MDA-MB-231 were grown to confluent monolayers on 6-well plates with parallel streaks in bottom. And vertical wounds were created by a pipette tip. Mitomycin C (Amresco) was used to inhibit cell viability. 1% FBS also was used in the assay. Progression of migration was observed and photographed at various times, four fixed fields were analyzed for each well. The percentage of inhibition was expressed using control wells at 100%. Wound images were taken with a digital camera mounted on light microscope. The wound gap widths were measured using Image J software.

2.7. Cell invasion assay

The cell invasion assay was carried out using a Transwell assay. The upper chamber of each 8.0 μm pore size Transwell apparatus (Corning, NY, USA) was coated with Matrigel (BD Biosciences, San Jose, CA). Breast cancer cells were added to the upper chamber at a density of $4*10^5$ cells/ml (100 μl per chamber) after starved overnight and incubated with different conditions and normal medium in the lower compartment. For 24 h of incubation, the cells on the upper surface were removed by a cotton swab. The invaded cells were fixed with 4% paraformaldehyde solution, stained with 0.1% crystal violet, and quantified by manual counting and ten randomly chosen fields were analyzed for each group.

2.8. Western blots

Cells were collected with lysis buffer after being washed three times with ice-cold PBS. Lysates were added WES automatic protein imprinted quantitative analysis system (Proteinsimple). The proteins were detected with specific antibodies. The quantification of the relative increase in protein expression and phosphorylation was performed using Compass software and was normalized with the control protein expression in each experiment.

2.9. Immunoprecipitation

293 T cells were transfected with control vector or Flag-DNER plasmid stimulated with or without PTN. 293 T cells lysates (1–2 mg of protein) were incubated 4 h at 4 °C with 2 μg of anti-FLAG monoclonal antibody (Sigma) followed by incubation with protein G-agarose beads (Invitrogen) at 4 °C for an additional 1 h. Beads were washed with 1 ml of wash buffer (4.3 mM Na_2HPO_4, 1.4 mM KH_2PO_4, pH 7.4, 137 mM NaCl, 2.7 mM KCl, 0.1% (*v*/v) Tween 20, 10 mM $MgCl_2$, 5 mM EDTA, 2 mM DTT), and the bound immune complexes were eluted by boiling in SDS sample buffer.

2.10. RNA isolation and Real-time PCR

According to manufacturer instructions, total RNA was extracted using TRIzol (Pufei, Shanghai) and cDNA was synthesized using the Reverse Transcript Kit (Promega). Real-time PCR was performed in triplicate using SYBR Green Master Mixture (TAKARA) on the Real-time PCR Detection System (Roche). Glyceraldehyde-3-phosphate dehydrogenase (GAPDH) was chose as an endogenous normalization control. The cycle threshold (Ct) value was used for quantification using the $2^{-\Delta\Delta Ct}$ method. Sequences of the primers are shown in the following Table S1.

2.11. Human samples and immunohistochemistry (IHC) staining

All procedures performed in studies involving human participants were in accordance with the ethical standards of the institutional research committee and with the 1964 Helsinki declaration and its later amendments or comparable ethical standards. Informed consent was obtained from all individual participants included in the study. A cohort of 126 paraffin-embedded human breast cancer specimens was diagnosed by histopathology at Renmin Hospital of Wuhan University from 2011 to 2012. The detailed clinicopathologic characteristics of the patients with breast cancer are shown in Table 1. The results of staining were evaluated and scored by two independent pathologists who were blinded to the clinical outcome, based on both the proportion of positively stained in cytoplasm and/or nucleus of tumor cells and the intensity of staining. The proportion of tumor cells was scored as: 0 (< 10% positive cells), 1 (10%–20% positive cells), 2 (21%–50% positive cells) and 3 (> 50% positive cells). The intensity of protein expression was determined as: 0 (no staining), 1 (weak staining, light brown), 2 (moderate staining, brown) and 3 (strong staining, dark brown). DNER staining positivity was determined using the following formula: overall score = percentage score × intensity score. The receiver operating characteristic analysis (ROC) was used to determine the optimal cut-off values of all antibodies expression levels for survival rate.

2.12. Quantum dots (QDs) - based fluorescent imaging technique

QDs-based fluorescent imaging technique has been established at our cancer center with detailed procedures reported previously. The QD-conjugated streptavidin (QD-SA) probe (1:200; QDs-605–goat F(ab) 2 anti-rabbit immunoglobulin G conjugate; Wuhan Jiayuan Quantum Dots Co. Ltd.) was used as the secondary antibody in the QD-based immunofluorescent imaging. Briefly, the sequence of the procedure was as follows: deparaffinizing, antigen retrieval, blocking (2% bovine serum albumin, 37 °C for 30 min), incubation with primary antibody (dilution 1:100, 37 °C for 2 h), washing, blocking, incubation with biotinylated secondary antibody (dilution 1:500, 37 °C for 30 min), washing, blocking, application of QD-SA 605 probes (dilution 1:200, 37 °C for 30 min, emitting red light), washing, mounting, and observation (Olympus BX51 fluorescence microscope; Olympus Corporation) with a blue light (wavelength of 450–490 nm) excitation.

Table 1
DNER and clinical characteristics of breast cancer patients.

Characteristic	DNER negative $N = 30$	DNER positive $N = 96$	P
Median RFS (months)	78	45	
Age, years			0.612
< 50	14	52	
≥ 50	16	44	
Grade			0.029
Well	0	2	
Moderately	16	18	
Poorly	14	76	
Tumor size			0.797
< 2 cm	8	22	
≥ 2 cm	22	74	
Lymph node metastasis			0.624
No	16	42	
Yes	14	54	
TNM stage			0.202
I	6	16	
II	16	30	
III	8	50	
ER			0.186
Positive	4	4	
Negative	26	92	
PR			0.018
Positive	6	2	
Negative	24	94	
HER2			0.193
Positive	6	12	
Negative	24	84	
Ki67			0.565
< 14%	20	56	
≥ 14%	10	40	

RFS: Recurrence-free survival, ER: estrogen receptor, PR: progesterone receptor, HER2: human epithelial growth factor receptor-2.

2.13. Immunofluorescence

For the analysis of DNER distribution in cells, we performed immunofluorescent multicolor staining. Sections were stained at room temperature for 1 h with a primary antibody. Antigen retrieval was performed in citrate buffer, pH 6.0. The blocking step was performed by incubating the slides with 5% bovine serum albumin (BSA) and endogenous biotin activity was quenched followed by incubation with rabbit antibody (Biorbyt, orb156622). The secondary biotinylated antibody (Abcam, ab150083) treatment was followed by Streptavidin-Alexa Fluor 594 conjugate (Life Technologies Molecular Probes, S32356). Slides were mounted in VECTASHIELD Antifade mounting medium containing DAPI (Vector Laboratories, H1200). Protein expression in cell sections were visualized using the Olympus FluoView FV1000b Confocal Microscope.

2.14. Lentivirus preparation and transfection

siRNA lentiviruses with 3 sequence targeting DNER (5′-ATGGGATCAAGTGGAGGTGAT-3′,5′-AAGGATACTTCGGATCTGCTT-3′,5′-CAGCAATGCCATTGCATCCAT-3′) were obtained from GeneChem Biotechnology (Shanghai, China), target sequences of human DNER (GeneBank accession no. NM_139072). MDA-MB-231 cells cultured at a density of 5×10^5 cells per 6 well plate. After incubated 24 h, the cells were transfected with DNER siRNA lentiviruses and control sequences using CON077 (GeneChem Biotechnology, China) following the manufacturer's instructions. Cell lysates were collected and RT-PCR were performed to detect mRNA expression using specific antibodies PCR data of three sequences are show in Fig. S3.

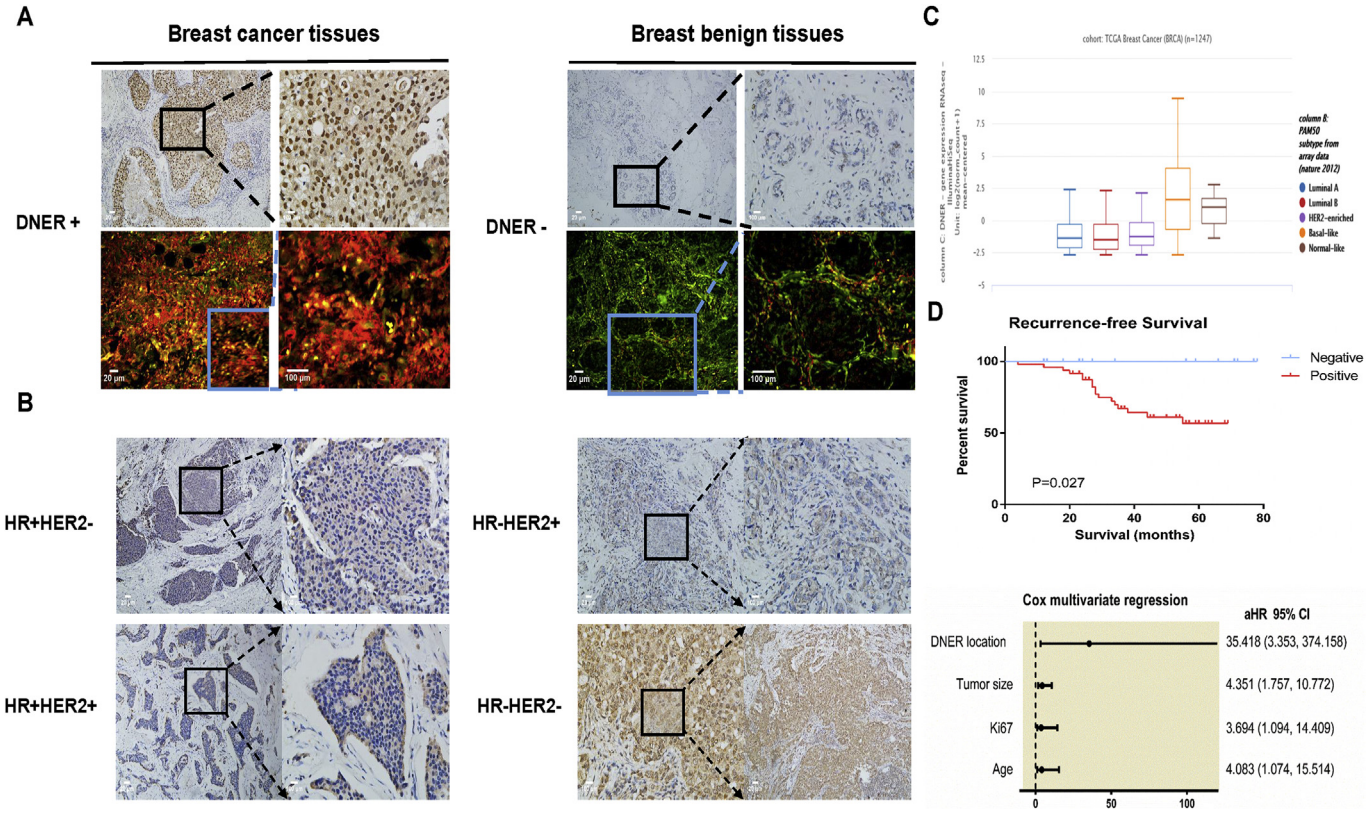

Fig. 1. DNER was overexpressed in triple-negative breast cancer and associated with poor prognosis of patients with breast cancer.
Immunohistochemistry and QD-based fluorescent imaging technique were performed using a DNER antibody. (A) DNER presented high expression in breast cancer and low expression in breast benign tissues. (B) DNER presented primarily high expression in breast cancer with hormone receptor (HR)- and HER2-negative subtype and low expression in other subtypes. (C) The box plot revealed the discrepancy of DNER expression in different subtypes of breast cancer. And the data derived from the TCGA. (D) Kaplan–Meier survival analysis showed that the RFS of DNER-negative patients was significantly better than that of DNER-positive patients (log-rank test $P = .027$), and patients with DNER up-regulating in cytoplasm/nucleus were likely to have a poorer RFS compared with those of DNER expression in membrane. Cox multivariate regression analysis indicated that DNER expression in cytoplasm/nucleus was an independent risk factor for breast cancer recurrence.

2.15. Xenograft tumor formation

Six-week-old female BALB/c nude mice were purchased from Vital River, Beijing. The animals were handled according to the protocol approved by the Institutional Animal Care and Use Committee of Renmin Hospital of Wuhan University. The following cell lines were used to create subcutaneous models: 2×10^6 MDA-MB-231 cells treated with control lentivirus or transfected with DNER knockdown lentivirus. All cell samples were subcutaneously injected with Matrigel (1:1), total volume 100 µl, into the axilla of the mice. Tumor volume was defined as (longest diameter) × (shortest diameter)^2/2 and was measured once every 5 days until day 25 using a Vernier calliper. After the mice were sacrificed, all tissues were collected, embedded in paraffin and stained with IHC or haematoxylin-eosin (HE).

2.16. Microarray

Total RNA was isolated using Trizol (Pufei, Shanghai) from three independent samples of the cells treated with control siRNA lentiviruses or DNER siRNA lentiviruses for 72 h. Affymetrix microarray was performed using the Human Gene 2.0 ST microarray chip. Data were normalized, significance determined by ANOVA, and fold change calculated with the Partek Genomics Suite. GO and PANTHER analyses were performed with DAVID for all differentially expressed genes (R ± 1.4-fold, $P < .05$), and GSEA was performed.

2.17. Statistical analysis

All statistical analyses and all charts of survival probabilities were performed with SPSS 22.0 (IBM Corporation, Armonk, NY, USA). The differences in the expression of DNER between breast cancer and benign disease tissue and the relationships between DNER and the baseline clinical characteristics of patients with breast cancer were evaluated by Chi-square test. The Kaplan–Meier method was used to calculate the patient survival probability and the log-rank test was used to assess the heterogeneity in the survival data for each prognostic factor. Multivariate Cox proportional hazard regressions were used to obtain hazard ratios (HRs) and their respective 95% confidence intervals to show the strength of the estimated relative risks. All experiments were done independently at least three times. Results are represented as the mean ± SD. Significant differences between two groups were analyzed by using an independent sample *t*-test. A *P*-value of < 0.05 was considered statistically significant.

3. Results

3.1. DNER was overexpressed in breast cancer tissue and associated with poor survival of patients with breast cancer

Firstly, we utilized immunohistochemistry to detect the expression of DNER in tissue samples of breast cancer and breast benign disease. It is evident that DNER protein indicated by brown staining was mainly expressed in cytoplasm and/or nucleus and scarcely in the plasma membrane. Therefore, positive DNER expression was defined as

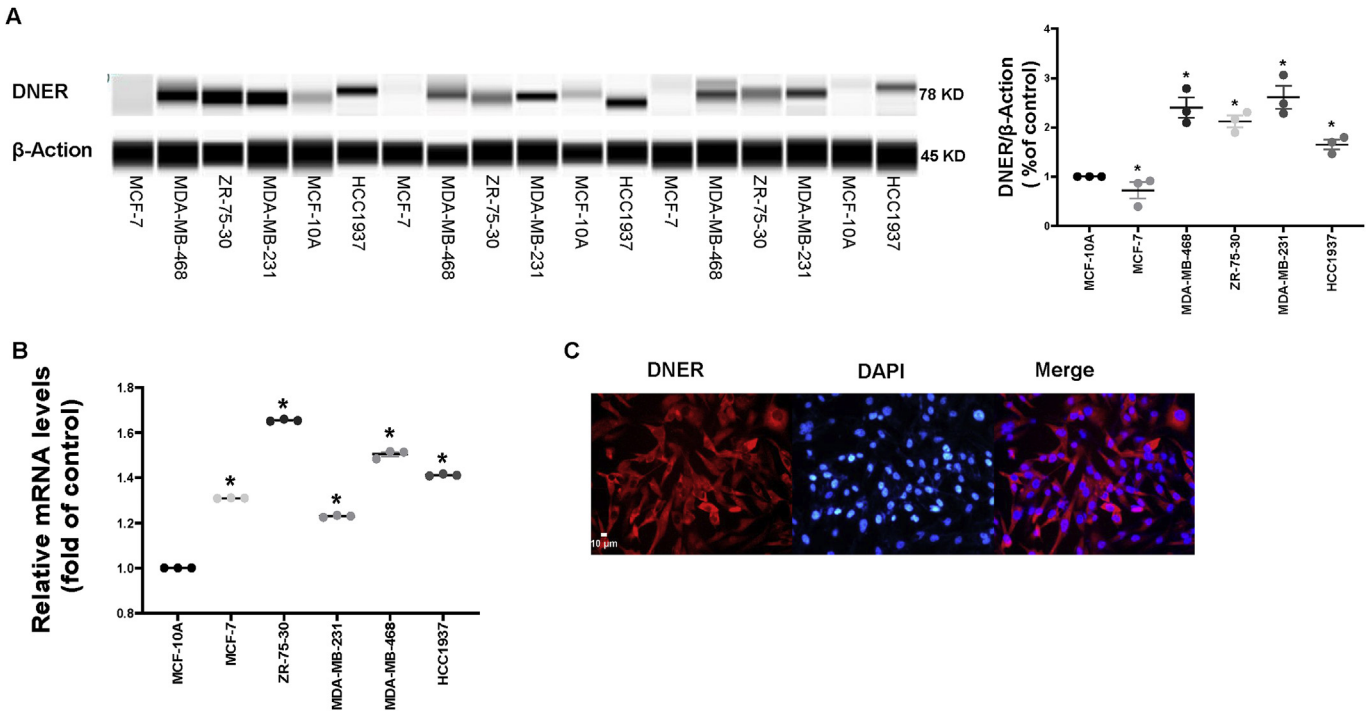

Fig. 2. The expression level of DNER was analyzed in breast cancer cell lines. (A) The protein expression of DNER was evaluated by western blot in breast cancer cell lines. (B) The mRNA expression of DNER was evaluated by RT-PCR in breast cancer cell lines. (C) The distribution of DNER in cells was detected by immunofluorescence (200×).

overexpression in cytoplasm and/or nucleus. Among the 126 breast cancer tissues, positive staining for DNER was observed in the samples from 96 patients, whereas only two patients exhibited positive DNER staining in 15 breast benign disease(Fig. 1A, Up). Further, the QD-based fluorescent imaging technique was adopted and the results showed that the red DNER signal was strong and primarily distributed on cellular nucleus in samples (Fig. 1A, Down). These results indicated that the expression of DNER was significantly higher in breast cancer tissues than in tissues obtained from patients with breast benign disease ($P < .01$, not shown).

Studies of the relationship between DNER expression and the clinical and pathological features of breast cancer patients have shown that the expression of DNER in patients with breast cancer was associated with the grade ($P = .029$) and revealed that the DNER positive rate increases with an increase in the tumor grade. In addition, the positive expression of DNER was more common in patients with the negative expression of progesterone receptor (PR) than those with PR positive ($P = .018$). No relationships were found between DNER and other clinical or pathological features, including age, tumor size, lymph node metastasis, TNM stage, estrogen receptor (ER), human epithelial growth factor receptor-2 (HER2) and Ki67 (Table 1). Therefore, the highest level of DNER was observed in breast cancer with triple-negative subtype (Fig. 1B), which was consistent with the data from The Cancer Genome Atlas (TCGA) (Fig. 1C). We analyzed the association between DNER and the prognosis of patients with breast cancer. The median recurrence-free survival (RFS) of breast cancer patients with positive DNER staining was 78 months compared with 45 months in patients with negative DNER. The Kaplan–Meier survival analysis showed that the RFS of patients with negative DNER staining was significantly longer than that of patients with positive DNER ($P = .027$; Fig. 1D). Furthermore, a Cox multivariate regression analysis also showed that the overexpression of DNER suggested a poor prognosis (aHR = 35.418, 95% CI: 3.353–374.158; Fig. 1D). The risk of death for DNER-positive patients was 35-fold greater than that for DNER-negative patients.

3.2. Effect of DNER on breast cancer cells viability, cell cycle, migration, invasion in vitro

The expression levels of DNER were determined by western blot and RT-PCR across mammary epithelial cell line (MCF-10A) and 5 breast cancer cell lines that encompass the known phenotypic heterogeneity. Interestingly, expression levels of DNER protein and mRNA were strikingly higher in 4 breast cancer cell lines than in MCF-10A cell line expect for MCF-7 cell ($P < .05$) (Fig. 2A–B). Taken together, MDA-MB-231 cell was chosen for the subsequent experiments. In addition, immunofluorescence analyses showed that DNER were distributed in cytoplasm/nuclear in MDA-MB-231 cell (Fig. 2C).

To investigate the effects of DNER-induced breast cancer cells growth, the knockdown expression of the DNER lentivirus vector was used to down-regulate the expression of DNER in MDA-MB-231 cells, and DNER overexpressed in MCF-7 cells via plasmid. MTT assays were performed to measure cell viability. As demonstrated in Fig. 3A, expression of DNER was positively related with viability of breast cancer cells. Down-regulated DNER impaired MDA-MB-231 cell viability while MCF-7 cells up-regulated DNER show more potential in cell viability. The results of flow cytometric methods also showed that the low expression of DNER increased the percentage of cells in S phase and reduced the fractions of cells in G1 and G2/M phases in MDA-MB-231 cells (Fig. 3B, Up). As for MCF-7 cells, we found that overexpression of DNER reduced the radio of S phase but elevated the proportion of G2/M phases (Fig. 3B, Down). We used wound healing and transwell assays as described in the materials and methods section to test the effect of DNER-induced breast cancer cells migration and invasion. As shown in (Fig. 3C), the wound was almost covered due to the influx of highly migratory cells in control group of MDA-MB-231 cells and the group of MCF-7 cells overexpression DNER, whereas the cells with low level of DNER expression groups remained close to the initial state. And transwell assays indicated that silencing DNER could significantly weaken the invasiveness of MDA-MB-231 cells (Fig. 3D, Up) and overexpression of DNER could enhance the potential of metastasis in MCF-7 cells (Fig. 3D, Down). Mice in the normal control group were

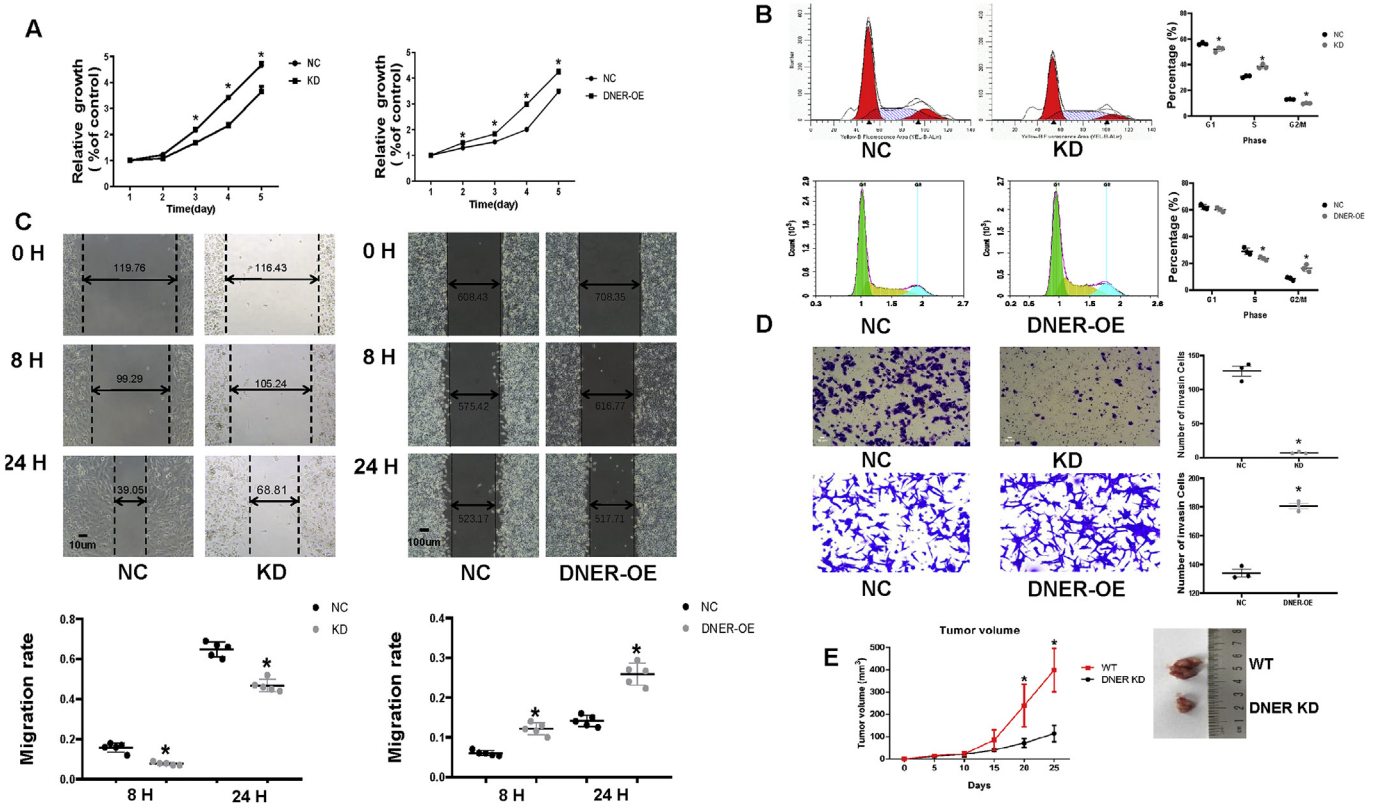

Fig. 3. DNER promotes breast cancer cell growth, migration, invasion.
DNER siRNA lentivirus was transfected into MDA-MB-231 cells and DNER overexpressed in MCF-7 cells via plasmid. (A). After selection the cells were plated in liquid culture conditions. Cell growth was measured by MTT assay until 5 days. (B) Cell cycle assay was used to examine the effects of DNER expression on cells cycle by flow cytometry analysis, and cell population (%) in each phase was quantified. (C). We transfected MDA-MB-231 cells with DNER siRNA or control siRNA and transfected MCF-7 cells with plasmid vectors of DNER overexpression or control plasmid vectors. Then detected changes in their motility using wound healing assay. The migration rate was correlated to cell migration ability. (D) Transwell assay was used to detect the effects of DNER on cells invasion. Changes in the number of cells penetrating the membrane in Transwell invasion assay. (E) DNER-knockdown or wild-type (WT) MDA-MB-231 cells were subcutaneously injected into the BALB/c nude mice (3 mice). Tumor size was measured every 5 days starting at day 25. Representative tumor images from 3 mice. The bars represent the mean values ± SD triplicate ($n = 3$). * $P < .05$, ** $P < .01$ versus control values. NC: control group, KD: DNER knockdown group.

injected with MDA-MB-231 cells and PBS, while those in the positive control group were injected with MDA-MB-231cells with DNER knockdown. We measured tumor volume for 25 days, and tumor growth was significantly decreased in mice injected with MDA-MB-231 cells undergoing DNER knockdown compared with those in the normal control group (Fig. 3E).

3.3. Analysis of potential mechanism of DNER in breast cancer

To gain further insights into molecular pathways perturbed by DNER knockdown, we performed Affymetrix microarray and assessed the global impact of DNER knockdown on MDA-MB-231 cells by transcriptional profiling, which consists of 883 up-related genes and 982 down-related genes in MDA-MB-231 cells with control siRNA compared to DNER knockdown (Fig. S1). Interestingly, pathway analysis using ingenuity pathway analysis (IPA) revealed that among top 10 statistically significant pathways (identification of > 10% genes in the pathway and –log (P value) > 4), seven pathways were associated with Interferon Signaling, Tight Junction Signaling, Role of CHK Proteins in Cell Cycle Checkpoint Control, Cell Cycle Regulation by BTG Family Proteins, Protein Ubiquitination Pathway and PI3K/AKT Signaling. While mRNA expression of CCDC88A (encoded Girdin), a positive regulator of the PI3K/AKT signaling pathway, was increased by overexpression of DNER, and mRNA expression levels of several key genes in the PI3K/AKT signaling pathway including PIK3R2, mTOR and RPS6KB1 were consistently increased (Fig. S1), suggesting that DNER up-regulated expression would activate the PI3K/AKT signaling pathway. Besides, interactive relationship between these pivotal regulatory factors were established and analyzed (Fig. S2).

3.4. DNER promotes PI3K/AKT activation through activating Girdin

To investigate whether the expression of Girdin was regulated by DNER in vitro, western blot and RT-PCR assays were used to detecting the protein and mRNA expression of Girdin, results of which indicating that protein and mRNA expression of Girdin in MDA-MB-231 cells exposed under DNER siRNA were not remarkably changed compared with those in control group (Fig. 4A–B). Moreover, the extent of p-Try for phosphotyrosine was determined by immunoblotting, suggesting that DNER knockdown reduced the tyrosine phosphorylation level (Fig. 4B). p85α and AKT from PI3K/AKT signaling pathway which are important effectors in tumor progression, are involved in the regulation of MDA-MB-231 growth, migration, invasion. Our results demonstrated that DNER knockdown downregulated the phosphorylation level of AKT at Ser473 and the expression of p85α that directly bound to the phosphotyrosines of Girdin, and then resulted in phosphorylating AKT at Ser473 [17] (Fig. 4B). Next, 293T cells overexpressing DNER were stimulated with PTN as described, DNER tyrosine phosphorylation was determined by Tyr(P) immunoblotting after DNER immunoprecipitation (Fig. 4D). To further characterize DNER tyrosine phosphorylation in response to PTN stimulation, we investigated its ability to bind Girdin. Immunofluorescence analyses showed that Both DNER and Girdin were distributed in cytoplasm/nuclear in MDA-MB-231 cell after PTN stimulation (Fig. 4C). We also found that purified DNER bound

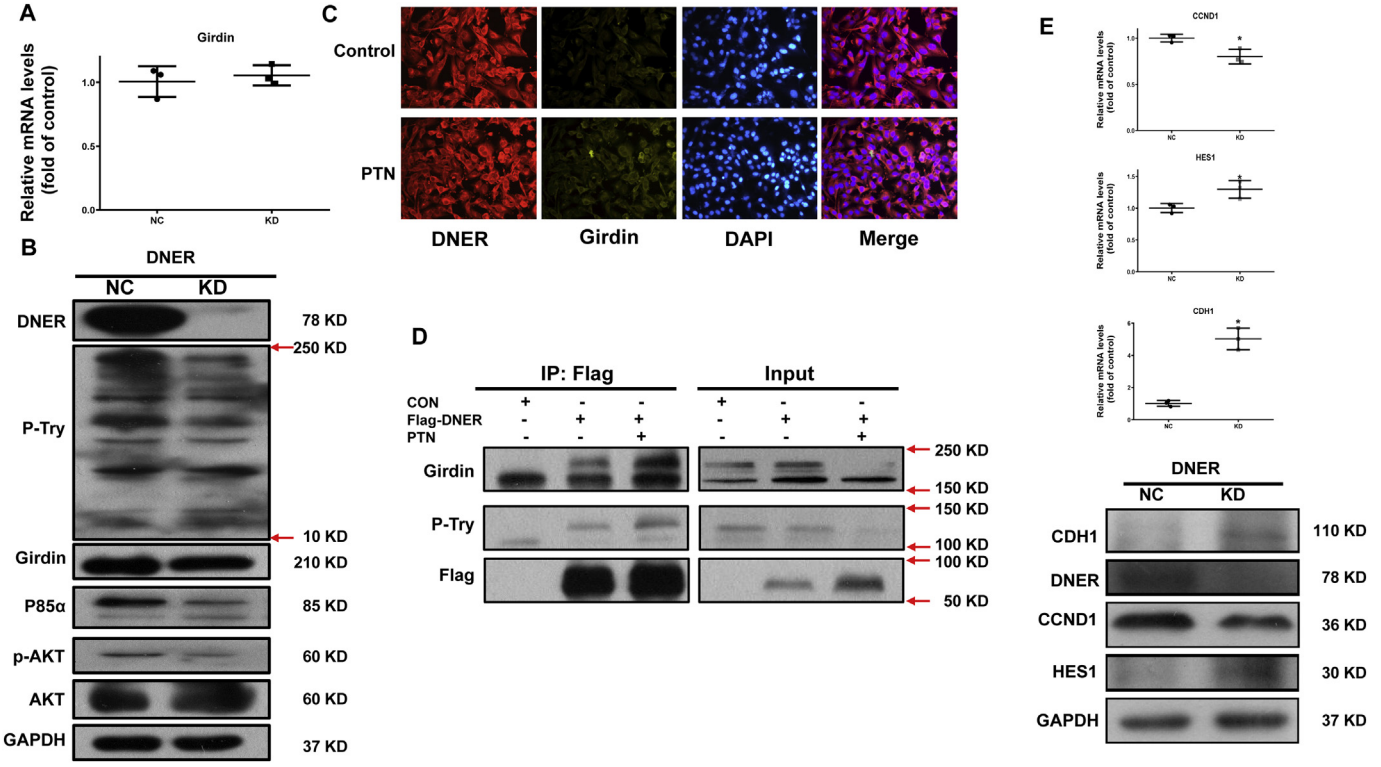

Fig. 4. DNER regulated breast cancer cell growth and invasion by Girdin/PI3K/AKT signaling and key regulatory genes.
(A) The mRNA level of Girdin didn't significantly reduce after DNER knockdown. (B) The silencing DNER significantly inhibited the expression of P85α, p-Try and p-AKT (Ser473). (C) qPCR data of CCND1, CDH1, HES1 and HEY1 expression in MDA-MB-231 cells transduced with lentiviruses carrying vectors with the DNER siRNA or empty vector (control). Expression values were normalized to genes expression in control cells was set to 100%. (D) The co-distribution of DNER and Girdin in cells was detected by immunofluorescence after PTN stimulation (200×). (E) 293 T cells expressing DNER-Flag or vector control (CON) were or stimulated with or without PTN, Flag immunoprecipitations were analyzed by western blot for P-Try and Girdin. The bars represent the mean values ± SD triplicate (n = 3). * P < .05, ** P < .01 versus control values. NC: control group, KD: DNER knockdown group.

over 2-fold more Girdin from 293T cells overexpressing DNER than from unstimulated controls while further increased after PTN stimulation (Fig. 4D). Therefore, the tyrosine-based sorting motif of DNER could be phosphorylated, and interact with Girdin to further activated PI3K/AKT signaling pathway.

As a Notch ligand, DNER had 10 EGF-like repeats in the extracellular domain closely relating to those of the developmentally important receptor Notch and its ligand Delta. It had been believed that ligand receptor binding mediated Notch signaling by stimulating cleavage of the Notch intracellular domain (NICD), and then NICD translocated to the nucleus, where it typically interacted with transcription factors to activate the transcription of target genes such as members of the Hes and Hey families involving in cell proliferation, differentiation and survival [18]. Taking into account that DNER was also a regular component of Notch signaling to promote cancer progression. The key regulatory genes were established to evaluate whether DNER would enhance tumor stemness. As the result of microarray, it demonstrated that CCND1 which play roles in cell cycle G1/S transition was the significantly downregulated in DNER knockdown group compared to control group. However, HES1 and CDH1 were remarkably upregulated. Meanwhile, Western Blots and RT-PCR assays were established to validate the protein and mRNA levels of these gene targets in cells expressing DNER or DNER knockdown, and the results were consistent with those of microarray (Fig. 4E). Meanwhile, we detected other genes such as MYC, Notch1 and Snail1, but their expression levels had no altered after DNER silence (not shown). Collectively, these data documented a role for DNER in maintaining the stemness and functional features of CSCs. Our data also demonstrate that DNER knockdown induced changes in CSCs genes expression profiles leading to reduced cell proliferation and migration. In conclusion, DNER could promote MDA-MB-231 cells growth and metastasis by activating Girdin/PI3K/AKT signaling pathway and modulate breast cancer cell stemness by targeting key genes, that provided a theoretical basis for future applications of DNER inhibitors in the treatment of breast cancer.

3.5. AKT mediated DNER-induced viability, migration, invasion of breast cancer cells

For further prove that DNER can promote breast cancer cells proliferation and metastasis by activating Girdin/PI3K/AKT signaling. SC79, a selective AKT activator which activates AKT phosphorylation [19], was used to investigate whether it reversed the suppression of silencing DNER in breast cancer cell. As demonstrated in Fig. 5A, after knockdown DNER, phosphorylation level of AKT at Ser473 was elevated after treated with SC79 whereas the expression of AKT was not changed, that means the activation of PI3K/AKT signaling pathway in the DNER knockdown MDA-MB-231 cells. Next, MTT assays indicated that cell viability of MDA-MB-231 silenced DNER was increased after treated with SC79 (Fig. 5B), and the results of flow cytometric methods showed that activating of AKT increased the percentage of cells in G1 and G2/M phases and reduced the fractions of cells in S phase in DNER knockdown MDA-MB-231 cells (Fig. 5C). Wound healing and transwell assays were used to detecting the effect of AKT activation induced migration and invasion in DNER knockdown MDA-MB-231 cells. As shown in Fig. 5D–E, SC79 could prominently promote the migration and invasion capabilities of MDA-MB-231 cells undergoing DNER silence.

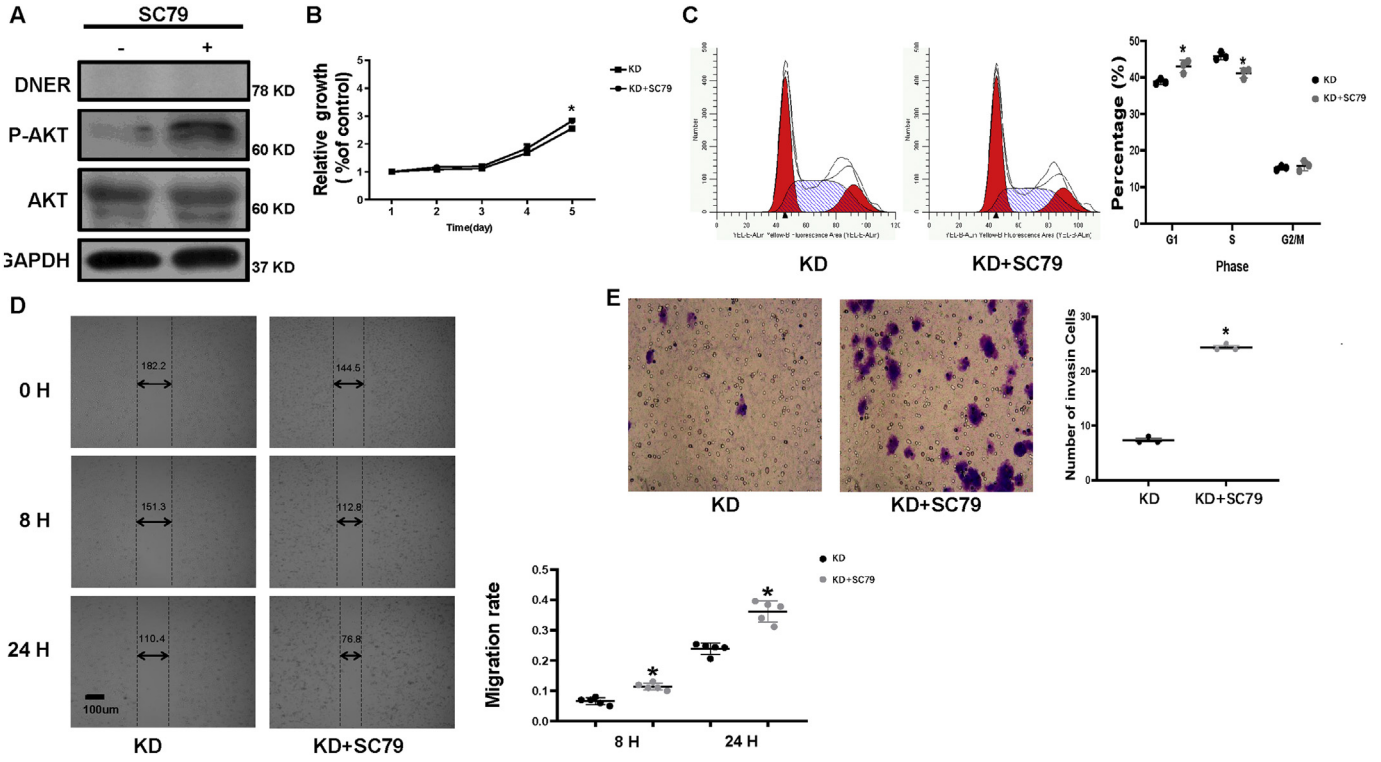

Fig. 5. AKT regulated the DNER-induced breast cancer cell growth and invasion.
(A) P-AKT (Ser473) was significantly increased in DNER knockdown MDA-MB-231 cells after SC79 stimulation. Whereas expression of AKT was not changed. (B) MTT assay was used to detect cell growth of DNER knockdown MDA-MB-231 cells with or without stimulated by SC79 until 5 days. (C) Cell cycle was measured by flow cytometry analysis to examine the effects of AKT activation on DNER knockdown MDA-MB-231 cells cycle, and cell population (%) in each phase was quantified. (D) We using wound healing assay to test the motility of DNER knockdown MDA-MB-231 cells. Compareing the migration of these cells with or without stimulated by SC79. (E) Transwell assay was used to detect the effects of AKT activation on DNER knockdown MDA-MB-231 cells invasion. Changes in the number of cells penetrating the membrane in Transwell invasion assay.

4. Discussion

In this study, we analyzed the role of DNER in proliferation and invasion of breast cancer and showed that a high expression of DNER in breast cancer were independently associated with poor RFS in breast cancer. In addition, our study demonstrated that DNER expression at both protein and mRNA levels was significantly high in MDA-MB-231 cells and DNER knockdown reduced viability, migration and invasion of MDA-MB-231 cells we also demonstrated that overexpression DNER in MCF-7 cells could highly increase cell viability, migration and invasion. Our findings also suggested that DNER activated PI3K/AKT axis via up-regulating expression of phosphorylated Girdin and orchestrated breast cancer cell stemness by targeting key genes, that is a promising therapeutic target and prognostic indicator in breast cancer.

DNER, a multidomain membrane protein, mediated cell–cell interaction as a Notch ligand [8]. DNER is expressed mainly in Purkinje cells of cerebellum, hippocampal neurons and glioblastoma cells [6,12,20]. The roles of DNER in cancer cell proliferation and migration have been previously explored. Sun et al. reported that DNER as a noncanonical Notch ligand could be induced by histone deacetylase (HDAC) inhibition that inhibited the growth of glioblastoma-derived neurospheres and growth as tumor xenografts, and induced their differentiation [12]. However, other studies had reached the opposite conclusion by demonstrated that the expression level of DNER both at mRNA and protein levels was comparatively high in several human cancer cell lines like Hela cells and PC3 cells, and DNER silencing significantly impaired cell transformation and reduced tumorigenicity in a cancer cells xenograft model [10]. The inconsistent or contrary results of these studies suggest that the effect of DNER may be tissue-specific, or the up-regulation of DNER by HDAC inhibition might be a kind of protective reaction. It had recently been shown that DNER knockdown significantly decreased the mRNA expression of Hey1 but had no effect on Hes1 expression [11,21]. However, our result showed that the mRNA and protein expression of Hes1 were unexpected to remarkably increase when DNER was silenced. Therefore, that DNER exerted a regulatory role in cancer progression was further required to be clarified.

Alternatively, it is also possible that DNER interacts with other signaling components as a receptor or a ligand. A unique aspect of the canonical DSL (Delta, Serrate, Lag2) ligands in Notch activation was their strict requirement for endocytosis, that ligand on the surface of a signal-sending cell must be internalized Notch ligands to activate Notch on the signal-receiving cell [22,23]. The structure of DNER had a tyrosine-based sorting motif in the cytoplasmic domain. Mototsugu et al. indicated that the coat-associated protein complex AP-1 directly bound to the tyrosine-based sorting motif of DNER and modulated subsequent function though the endocytosis system in vivo, that explained the reason why DNER was found to overexpress in endosomes [7]. In addition, our results indicated that silencing DNER significantly reduced CCDC88A gene, that encoded Girdin protein, and down-regulated the expression of phosphorylated AKT at 473. It reported that both phosphorylation of epidermal growth factor receptor (EGFR) and activation of G-protein coupled receptors (GPCRs) resulted in tyrosine phosphorylation of Girdin at Tyr^{1764} and Tyr^{1798}, that directly bound to the SH2 domains of the regulatory p85α-subunit of PI3K and enhanced AKT activity though triggering the activation of PI3K [17,24,25]. It was possible that DNER might be phosphorylated in a tyrosine-based sorting motif in the cytoplasmic domain, and then activated Girdin/PI3K/AKT signaling pathway. Therefore, the mechanism of DNER involving in the phosphorylation and endocytosis in cancer growth and metastasis were supposed to be further investigated.

5. Conclusions

In summary, DNER could promote breast cancer growth and metastasis by activating Girdin/PI3K/AKT signaling pathway and modulate breast cancer cell stemness by targeting key genes, that provided a theoretical basis for future applications of DNER inhibitors in the treatment of breast cancer.

Supplementary data to this article can be found online at https://doi.org/10.1016/j.cellsig.2019.109389.

Declaration of Competing Interest

The authors declare no conflict of interest.

Acknowledgments

We thank a professional English editor (American Journal Experts) for assistance in improving the quality of language. This work was partially supported by a National Natural Science Foundation of China (NSFC) grant (Grant NO: 81471781) and a National Major Scientific Instruments and Equipment Development Projects (Grant NO: 2012YQ160203) to Dr. Shengrong Sun, an NSFC grant to Dr. Juanjuan Li (Grant NO: 81302314), an NSFC grant to Prof. Changhua Wang (Grant NO: 81870550), and Hubei Province Health and Family Planning Scientific Research Project (RMYD2018M78) to Dr. Sun Si and a Fundamental Research Funds for the Central Universities of China grant (Grant NO: 2042019kf0102) to Dr. Wang Li Jun.

References

[1] W. Chen, R. Zheng, P.D. Baade, S. Zhang, H. Zeng, F. Bray, A. Jemal, X.Q. Yu, J. He, CA Cancer J. Clin. 66 (2016) 115–132.
[2] N. Takebe, L. Miele, P.J. Harris, W. Jeong, H. Bando, M. Kahn, S.X. Yang, S.P. Ivy, Nat. Rev. Clin. Oncol. 12 (2015) 445–464.
[3] A. Califano, M.J. Alvarez, Nat. Rev. Cancer (2016), https://doi.org/10.1038/nrc.2016.124.
[4] M. Reedijk, Adv. Exp. Med. Biol. 727 (2012) 241–257.
[5] V. Bolos, E. Mira, B. Martinez-Poveda, G. Luxan, M. Canamero, A.C. Martinez, S. Manes, J.L. de la Pompa, Breast Cancer Res. 15 (2013) R54.
[6] S.Y. Saito, H. Takeshima, Cerebellum. 5 (2006) 227–231.
[7] M. Eiraku, Y. Hirata, H. Takeshima, T. Hirano, M. Kengaku, J. Biol. Chem. 277 (2002) 25400–25407.
[8] M. Eiraku, A. Tohgo, K. Ono, M. Kaneko, K. Fujishima, T. Hirano, M. Kengaku, Nat. Neurosci. 8 (2005) 873–880.
[9] V.C. Luca, K.M. Jude, N.W. Pierce, M.V. Nachury, S. Fischer, K.C. Garcia, Science. 347 (2015) 847–853.
[10] D.-H. Yu, R. Sundaram, V. Nguy, W. Fan, S. Long, H. Ma, F. Wong-Staal, H.Q.X. Li, Cancer Res. 66 (2006) 767.
[11] L. Wang, Q. Wu, S. Zhu, Z. Li, J. Yuan, D. Yu, Z. Xu, J. Li, S. Sun, C. Wang, Am. J. Transl. Res. 9 (2017) 5031–5039.
[12] P. Sun, S. Xia, B. Lal, C.G. Eberhart, A. Quinones-Hinojosa, J. Maciaczyk, W. Matsui, F. Dimeco, S.M. Piccirillo, A.L. Vescovi, J. Laterra, Stem Cells 27 (2009) 1473–1486.
[13] A. Enomoto, H. Murakami, N. Asai, N. Morone, T. Watanabe, K. Kawai, Y. Murakumo, J. Usukura, K. Kaibuchi, M. Takahashi, Dev. Cell 9 (2005) 389–402.
[14] P. Ghosh, A.O. Beas, S.J. Bornheimer, M. Garcia-Marcos, E.P. Forry, C. Johannson, J. Ear, B.H. Jung, B. Cabrera, J.M. Carethers, M.G. Farquhar, Mol. Biol. Cell 21 (2010) 2338–2354.
[15] M. Garcia-Marcos, J. Ear, M.G. Farquhar, P. Ghosh, Mol. Biol. Cell 22 (2011) 673–686.
[16] T. Kitamura, N. Asai, A. Enomoto, K. Maeda, T. Kato, M. Ishida, P. Jiang, T. Watanabe, J. Usukura, T. Kondo, F. Costantini, T. Murohara, M. Takahashi, Nat. Cell Biol. 10 (2008) 329–337.
[17] C. Lin, J. Ear, Y. Pavlova, Y. Mittal, I. Kufareva, M. Ghassemian, R. Abagyan, M. Garcia-Marcos, P. Ghosh, Sci. Signal. 4 (2011) ra64.
[18] E.R. Andersson, U. Lendahl, Nat. Rev. Drug Discov. 13 (2014) 357–378.
[19] H. Jo, S. Mondal, D. Tan, E. Nagata, S. Takizawa, A.K. Sharma, Q. Hou, K. Shanmugasundaram, A. Prasad, J.K. Tung, A.O. Tejeda, H. Man, A.C. Rigby, H.R. Luo, Proc. Natl. Acad. Sci. U. S. A. 109 (2012) 10581–10586.
[20] J. Kurisu, T. Fukuda, S. Yokoyama, T. Hirano, M. Kengaku, J. Neurochem. 113 (2010) 1598–1610.
[21] L. Wang, Q. Wu, S. Zhu, Z. Li, J. Yuan, L. Liu, D. Yu, Z. Xu, J. Li, S. Sun, Cancer Biomark. (2018) 1–9.
[22] B. D'Souza, A. Miyamoto, G. Weinmaster, Oncogene. 27 (2008) 5148–5167.
[23] J.T. Nichols, A. Miyamoto, G. Weinmaster, Traffic. 8 (2007) 959–969.
[24] A. Leyme, A. Marivin, M. Garcia-Marcos, J. Biol. Chem. 291 (2016) 8269–8282.
[25] I. Lopez-Sanchez, Y. Dunkel, Y.S. Roh, Y. Mittal, S. De Minicis, A. Muranyi, S. Singh, K. Shanmugam, N. Aroonsakool, F. Murray, S.B. Ho, E. Seki, D.A. Brenner, P. Ghosh, Nat. Commun. 5 (2014) 4451.